Biophysical Properties of Human Erythrocyte Spectrin at Alkaline pH: Implications for Spectrin Structure, Function, and Association†

Takashi Fujita,‡ Gregory B. Ralston,‡ and Michael B. Morris*,§

Departments of Biochemistry and Pharmacy, University of Sydney, Sydney NSW 2006, Australia

Received August 8, 1997; Revised Manuscript Received October 20, 1997⊗

ABSTRACT: The effects of pH 6−13 on the conformation and assembly of spectrin were studied by means of analytical ultracentrifugation, circular dichroism (CD), ^{1}H NMR, and UV spectrophotometry. Sedimentation velocity analysis showed that spectrin oligomers dissociate cooperatively into component α- and β-subunits above pH 9.5, and that spectrin tetramers, heterodimers, and monomers adopt more extended and/or expanded shapes above this pH. The dissociation to monomers is mostly completed by pH 10.5 and is used as the basis for purifying the subunits [see Fujita *et al*. (1998) *Biochemistry 37*, 272−280]. Along with the dissociation, biphasic unfolding of spectrin was observed above pH 9.5 as detected by CD. The first phase of the transition occurred between pH 9.5 and 11, and the second phase between pH 11 and 13. A similar biphasic dependence was observed for the upfield shift of lysine ϵ-CH_2 resonances detected by spin-echo ^{1}H NMR and the spectrophotometric titration of the absorbance at 294 nm. These data indicate that deprotonation of tyrosine and lysine residues is closely correlated with (i) the dissociation of spectrin oligomers into heterodimers, (ii) the dissociation of heterodimers into monomers, and (iii) the unfolding of spectrin. Taken together, our data suggest that hydrophobic and electrostatic interactions involving tyrosine and lysine residues play a critical role in the formation of the α-helix of spectrin and assembly of physiologically relevant spectrin oligomers from the two component subunits.

Erythrocyte spectrin is the major component of the red-cell cytoskeleton, the two-dimensional meshwork of proteins underlying the cytoplasmic face of the lipid bilayer (*1*). The inherent flexibility of spectrin is believed to be a major contributor to the elastic deformability displayed by red cells during their passage through the circulatory system (*2*, *3*). Spectrin is composed of a 280 kDa α-subunit (*4*) and a 246 kDa β-subunit (*5*) which associate laterally in an antiparallel orientation (*6*) to form a two-stranded (*7*), highly elongated, wormlike heterodimer (*8*). The α- and β-subunits consist largely of a series of 106 amino acid repeat motifs (20 and 16 complete repeats, respectively) with each repeat predicted to fold into a triple-helical bundle (*4*, *5*, *9*, *10*). An X-ray structure of a single repeat motif shows that the triple-helical bundle is stabilized both by extensive hydrophobic interactions between the interior faces of the amphipathic helices and by electrostatic interactions between the charged residues on the exterior surface (*9*).

The heterodimers self-associate in a "head-to-head" fashion to form tetramers (the dominant form in the membrane skeleton) and higher-order oligomers (*11*). The self-association involves complementary binding sites near the C-terminus of the β-subunit and the N-terminus of the α-subunit. In particular, the 17th repeat of the β-subunit is incomplete and contains only helices 1 and 2 of the triple-helical bundle (nomenclature of Speicher *et al*. (*12*)). This partial repeat can combine with the N-terminal partial repeat of the α-subunit, which contains only helix 3, to form the complete three-helix bundle (*12*, *13*).

Liu *et al.* (*11*) examined the effects of alkaline pH and urea on spectrin extraction from erythrocyte membrane skeletons. Extraction of spectrin oligomers from the cytoskeletal network was reported at pH > 9. At pH ≥ 11.5, most of the extracted spectrin had dissociated into spectrin dimers, as determined by nondenaturing gel electrophoresis performed at neutral pH. Spectrin oligomers were released from the cytoskeletal network in 1−2 M urea and the protein network was completely disrupted in 4 M urea. Liu and colleagues mentioned the possibility of dissociation of spectrin α- and β-subunits at high pH and at high urea concentration. The dissociation might have occurred prior to the nondenaturing gel electrophoresis of their samples which was performed at neutral pH without urea. In fact, 3 M urea is now used for isolation of spectrin subunits (*14*).

The effectiveness of alkaline pH on extraction of spectrin from erythrocyte ghosts could result from deprotonation of amino acid side chains which stabilize intramolecular interactions within spectrin itself. For example, the possible importance of the residue at A7 (residue 7 of helix A, based on the labeling used by Yan *et al.* (*9*)), which is usually Tyr or Phe, was pointed out in the X-ray crystallographic study

† This work was supported by an Australian Research Council Large Grant to G.B.R., Overseas Postgraduate Research Scholarship and University of Sydney Postgraduate Research Scholarship to T.F., and a Ramaciotti Foundation Grant to M.B.M.

* Author to whom correspondence should be addressed. Telephone: 61-2-9351-2359. Fax: 61-2-9351-4391. E-mail: michaelm@pharm.usyd.edu.au.

‡ Department of Biochemistry, University of Sydney.

§ Department of Pharmacy, University of Sydney.

⊗ Abstract published in *Advance ACS Abstracts,* December 1, 1997.

S0006-2960(97)01966-1 CCC: $15.00
Published on Web 01/06/1998

of a spectrin repeat (*9*). This residue maintains contacts between the straight helix A and the coiled helices B and C. In addition to this and other hydrophobic interactions involving tyrosines, electrostatic interactions between Asp at A28, Lys at B7, and Lys at C25 also appear to stabilize the structure of the triple-helical bundle (*9*). Since all spectrin repeats are predicted to have a similar three-helix packing (*9*), deprotonation of tyrosine and lysine residues at alkaline pH will most likely result in destabilization of the folding of these repeat segments.

In this report, we investigated the effects of alkaline pH on the conformation, assembly, and self-association of spectrin using analytical ultracentrifugation, circular dichroism, ^{1}H NMR, and UV spectrophotometry. We found that the spectrin oligomers dissociate into individual α- and *β*-subunits above pH 9.5. The dissociation of spectrin oligomers to smaller species was accompanied by loss of α-helix and correlates with deprotonation of tyrosine and lysine residues. These results suggest that tyrosine and lysine residues play an important role in stabilizing the triple-helical bundles of spectrin, in the formation of heterodimers from α- and *β*-subunits, and in the self-association to tetramers and larger oligomers.

MATERIALS AND METHODS

Purification of Spectrin Dimers. Packed human red cells, prepared from blood drawn from normal, healthy donors, were obtained from Red Cross Transfusion Service, Sydney, Australia, and were used within 48 h of collection. Spectrin heterodimer was extracted from the cells, and the vesicles were removed by centrifugation, essentially as described previously (*15*). Following extraction, the crude extract of spectrin heterodimer was concentrated with Aquacide II (Calbiochem) to 20−30 mg/mL and dialyzed against buffer C (10 mM sodium phosphate, 100 mM NaCl, 5 mM EDTA, 0.1 mM DTT,[1] 0.3 mM PMSF, and 0.02% NaN_3, pH 7.5) for 2−3 h. The extract was then clarified by centrifugation at 48 000*g* for 10 min.

Spectrin was purified from the clarified extract using a Sepharose CL-4B column (2.5 cm × 55 cm) which had been pre-equilibrated with buffer C as described previously (*15*). The spectrin heterodimer fractions were pooled and concentrated with Aquacide III (Calbiochem) and rechromatographed in the same manner. Fractions from the spectrin dimer peak were pooled and used for experimentation as soon as possible to minimize the degradation of spectrin due to proteolysis.

Preparation of Samples for Analytical Ultracentrifugation, Circular Dichroism, and UV Spectrophotometric Measurements. Purified spectrin was dialyzed overnight at 4 °C against 5 mM sodium phosphate (pH 7.5), 0.1 mM DTT plus either 100 mM NaCl (for UV spectrophotometry and analytical ultracentrifugation) or 100 mM NaF (for CD). Samples were clarified by centrifugation at 48 000*g* for 10 min. The pH of each spectrin sample was adjusted by diluting the stock spectrin solutions (∼2 mg/mL) about 20-fold in a buffer comprised of 50 mM sodium phosphate, 50 mM sodium borate, 70 mM NaCl (or NaF for CD studies), and 0.1 mM DTT which was pre-adjusted to the desired pH (*16*). Spectrin concentrations were determined from the absorbance at 280 nm using an extinction coefficient of $E_{1g/L,1cm} = 1.14$, which we calculated from the amino acid composition (*4*, *5*) according to the method of Gill and von Hippel (*17*). This value of the extinction coefficient is in agreement with the value experimentally determined by Ralston (*18*).

Preparation of Samples for NMR Measurements. Purified spectrin was concentrated to ∼20 mg/mL by dialysis against Aquacide II. The concentrated sample was dialyzed against 1 mM sodium phosphate (pH 7.5) with 0.1 mM DTT for 3 h. The spectrin was then dialyzed three times (∼24 h total) against D_2O (99.75%; ANSTO, Lucas Heights, Sydney) containing 1 mM sodium phosphate (pH_{app} 7.2 at 20 °C; readings were uncorrected for the presence of D_2O). All D_2O buffers were purged with nitrogen to remove dissolved oxygen. The dialyzed spectrin was clarified by centrifugation at 48 000*g* for 10 min. The spectrin (∼0.1 mL) was then diluted into 4 volumes of 100 mM sodium phosphate and 100 mM sodium borate in D_2O which was pre-adjusted to the desired pH_{app} and placed into a 5 mm-diameter NMR tube. The final protein concentration was ∼4 mg/mL.

Acquisition and Processing of ^{1}H NMR Data. ^{1}H NMR spectra of spectrin were acquired at 20 °C and processed as described previously (*15*) using a Bruker AMX 400 MHz wide-bore spectrometer, operating in the pulsed Fourier transform mode. A CPMG pulse sequence was used to acquire spectra without water presaturation (*19*). A total echo time, *τ*, of 2 ms was used and was sufficient to remove the broad envelope arising from highly immobile protons; 16K data points were collected, the spectral width was 8.9 kHz, and 128 acquisitions were co-added. The total delay between the start of each acquisition was 5 s, which allowed for full relaxation.

Sedimentation Velocity Experiments. Sedimentation velocity experiments were performed using a Beckman Optima XL-A analytical ultracentrifuge at 20 °C. Sample concentrations were 0.1 g/L in all experiments. The spectrin samples (400 μL) and buffer against which the protein had been dialyzed (420 μL) were placed in cells fitted with double-sector centerpieces and quartz windows. The samples were centrifuged at speeds ranging from 42 000 to 49 000 rpm, depending on the pH of the sample. Ten scans were acquired at 230 nm at 15 min intervals using the continuous scan mode, a step size of 0.005 cm, and 5 readings averaged per step. When there were window defects or partial masking, scans at 230 nm were corrected by subtracting the scans at 360 nm which were collected at 3000 rpm at the beginning of the experiment.

The data were analyzed using the program SVEDBERG (*20*). Up to 9 raw scans were directly fitted with an approximate solution of the Lamm equation using nonlinear least-squares techniques to return values of the diffusion coefficient and sedimentation coefficient for up to 3 species. A zero offset (non-zero absorbance at zero solute concentration) was also included as a fitting parameter when necessary. The program also returns the percentage, by weight, of each of the species, and the molecular weights of the species were calculated in the program using the following equation (*21*):

[1] Abbreviations: $[\theta]_{MRW}$, mean residue ellipticity; $[\theta]_{222}$, mean residue ellipticity at 222 nm; A_{230}, absorbance at 230 nm; A_{294}, absorbance at 294 nm; CPMG, Carr−Purcell−Meiboon−Gill; DTT, dithiothreitol; pH_{app}, apparent pH; PMSF, phenylmethanesulfonyl fluoride; $s_{20,w}$, sedimentation coefficient corrected to water at 20 °C.

$$M = sRT/D(1 - \rho\bar{\nu}) \quad (1)$$

where M is the molecular weight of the protein, $\bar{\nu}$ (mL/g) is the partial specific volume of the protein, ρ (g/mL) is the solvent density, s (S) is the sedimentation coefficient, D (cm^2 s^{-1}) is the diffusion coefficient, R is the gas constant, and T (K) is the absolute temperature.

UV Spectrophotometry. Spectrophotometric measurements of spectrin were performed using a Hewlett-Packard 8452A diode array spectrophotometer at temperatures of 10−30 °C. Absorbance of spectrin samples was measured at 294 nm in a 1 cm quartz cell in which the temperature was controlled using a HP89054A thermostatable cell holder. Correction for light scattering was made by measuring the absorbance at 360 nm and subtracting this value from the absorbance at 294 nm. The correction was always less than 5% of the value at 294 nm.

When the reversibility of the pH dependence of the absorbance at 294 nm of spectrin was examined, the titration was performed at 20 °C in a 10 mL beaker containing 0.1 g/L spectrin, 50 mM sodium phosphate, 50 mM sodium borate, 70 mM NaCl, and 0.1 mM DTT, in which a pH electrode was directly inserted. The pH of the sample was changed by adding aliquots of 5 M NaOH and 5 M HCl while the solution was stirred using a magnetic stirrer. Samples (500 μL) of the spectrin solution were collected at the desired pH values, and the absorbance at 294 nm was measured as described above. The volumes of the added NaOH and HCl and that of the collected sample for each measurement were recorded, and the measured absorbance was corrected for dilution.

Circular Dichroism Measurements. Circular dichroism spectra were obtained with a Jasco J-720 spectropolarimeter at 20 °C. Samples of spectrin (0.1 g/L) were placed in a 1 mm cell, and scans were taken between 260 and 180 nm at a scan speed of 20 nm/min with response time of 1 s, band width of 1.0 nm, resolution of 0.5 nm, and sensitivity of 100 mdeg. Four acquisitions were co-added, and the spectra of buffer obtained in the same way were subtracted from the sample spectra. The raw data were converted to mean residue ellipticity ($[\theta]_{MRW}$), using a mean residue weight of 115.2 which we calculated from the cDNA sequence (*4*, *5*).

Analysis of the pH Titration Data. pH titration data from UV spectrophotometry were plotted as a function of pH and analyzed in the following manner. We assumed that the prototropic spectrin can exist in up to three states, A, B, and C, each allowed to have different absorbance coefficients. The pH-dependent equilibria were expressed as follows:

$$A \rightleftharpoons B + mH^+ \qquad K_1 = bx^m/a \quad (2)$$

$$B \rightleftharpoons C + nH^+ \qquad K_2 = cx^n/b \quad (3)$$

where a, b, c, and x are the molar concentrations of A, B, C, and H^+, respectively; m and n are the cooperativity coefficients, which correspond to the number of titratable groups per unit at each step; and K_1 and K_2 are the equilibrium constants for the first and the second transition, respectively. From the definition of K_1 and K_2, fractions of a, b, and c of the total concentration C_t can be calculated as follows:

$$a/C_t = x^{(m+n)}/(x^{(m+n)} + K_1x^n + K_1K_2) \quad (4)$$

$$b/C_t = K_1x^n/(x^{(m+n)} + K_1x^n + K_1K_2) \quad (5)$$

$$c/C_t = K_1K_2/(x^{(m+n)} + K_1x^n + K_1K_2) \quad (6)$$

The absorbance y can be expressed as

$$y = a\epsilon_a + b\epsilon_b + c\epsilon_c \quad (7)$$

where ϵ_a, ϵ_b, and ϵ_c are the absorbance coefficients of A, B, and C, respectively. Thus, the equation with which the data were fitted by nonlinear regression is

$$y = (x^{(m+n)}e_1 + K_1x^me_2 + K_1K_2e_3)/(x^{(m+n)} + K_1x^m + K_1K_2) \quad (8)$$

where y is the absorbance at a pH of $-\log x$, and $e_1 = c_t{\cdot}\epsilon_a$, $e_2 = c_t{\cdot}\epsilon_b$, and $e_3 = c_t{\cdot}\epsilon_c$ are the absorbances of the sample before the first transition, after the first transition, and after the second transition, respectively.

Analogous equations were used to fit pH titration data obtained from the CD, analytical ultracentrifuge, and ^1H NMR experiments.

The appropriateness of the model was examined by F-test in which F was calculated from the following equation (*22*):

$$F = (R_2 - R_1)(q - p_1)/R_1(p_1 - p_2) \quad (9)$$

where R_1 and p_1 are the sum of squares of the residuals and the number of parameters associated with the more complex model, respectively. R_2 and p_2 are the corresponding values of the simpler model, and q is the number of data points. The degrees of freedom of F are $(p_1 - p_2)$ and $(q - p_1)$. In all cases, comparison between single transition models and double transition models gave F values that would be obtained by chance with less than 5% probability, which indicates that the double transition models provided a significantly better fit to the data. The exception was the pH dependence of the proportion of spectrin monomers, which was better fitted by a single cooperative transition model. Significant improvement of the fits was not obtained by using a three-step transition model as determined by the F-test.

RESULTS

pH Dependence of the Sedimentation of Spectrin. Figure 1A shows the pH dependence of the sedimentation coefficient ($s_{20,w}$) of spectrin species over the pH range 6−13 at 20 °C. In our preparations, the tetramer content was consistently ∼20% at 20 °C, pH 7.5, at a spectrin concentration of 0.1 g/L. Sedimentation coefficients of both the tetramer and heterodimer decreased with increasing pH, indicating that the hydrodynamic shape of spectrin became increasingly asymmetric or expanded. Above pH 9.5, species with a sedimentation coefficient of ∼6 S and calculated molecular mass of ∼220 kDa appeared, indicating that the heterodimers began to dissociate into α- and β-subunits. The proportions of the various spectrin species vs pH are shown in Figure 1B. The proportion of spectrin monomers increased cooperatively with increasing pH above 9.5, and the monomer subunits were the predominant species at pH ≥ 10.5.

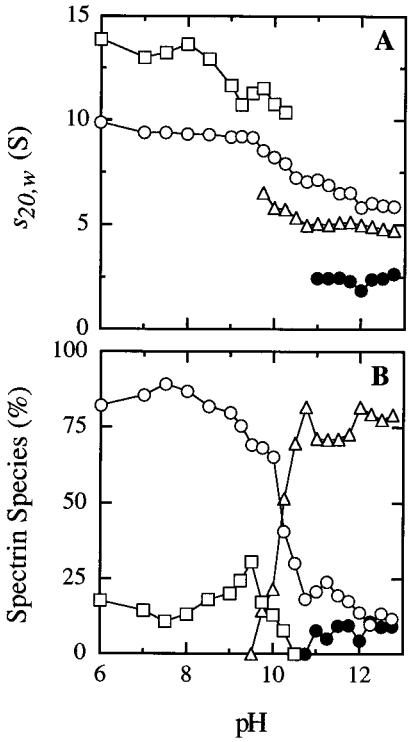

FIGURE 1: Effect of pH on the conformation of human erythrocyte spectrin. (A) pH dependence of the sedimentation coefficients of spectrin species at 20 °C. Spectrin (~2 g/L, pH 7.5) was diluted to 0.1 g/L in a buffer comprised of 50 mM sodium phosphate, 50 mM sodium borate, 70 mM NaCl, and 0.1 mM DTT which was pre-adjusted to the desired pH (*16*). The samples were centrifuged at 42 000−49 000 rpm, and scans were collected every 15 min at a wavelength of 230 nm. Sedimentation coefficients for up to 3 species were calculated using the program SVEDBERG (*20*). (B) The proportions of various spectrin oligomers and monomers vs pH for the same set of experiments shown in panel A. Values were calculated using the program SVEDBERG (*20*). Symbols represent spectrin tetramer (□), dimer (○), monomers (△), and grossly unfolded or degraded protein (●).

Tetramers were not detectable above pH 10.25. At pH ≥ 11, a boundary with a sedimentation coefficient of ~2.5 S appeared (Figure 1A,B). This may represent a degraded product of spectrin or highly asymmetric or expanded molecules.

The pH dependence of the sedimentation coefficient of the spectrin dimer and the proportion of monomers was fitted with eq 8 as shown in Figure 2A. For the proportion of monomers, a single cooperative transition model ($m = 2$) adequately fitted the data. For the sedimentation coefficient of dimers, a double cooperative transition model ($m = 2$, $n = 2$) was required to fit the data adequately. The returned values of apparent pK_a, where the values of pK_a are the midpoints of the transitions, are listed in Table 1.

pH-Dependent Unfolding of Spectrin Detected by CD. A set of CD spectra of spectrin obtained at various pH values at 20 °C is shown in Figure 3. The mean residue ellipticity at 222 nm ($[\theta]_{222}$) of spectrin was plotted over the range pH 7−13 in order to follow the change in α-helicity of spectrin (*23*). The pH dependence was fitted using eq 8 as shown in Figure 2B. The magnitude of the CD ellipticity decreased with increasing pH above pH 9.5, indicating a loss of α-helix and hence unfolding of the molecule. The pH dependence of the ellipticity could be fitted adequately assuming two cooperative transitions ($m = 2$, $n = 2$) and is similar to the pH dependence of the sedimentation coefficient of spectrin heterodimer (Figure 2A). The returned values of apparent pK_a are listed in Table 1.

Table 1: Apparent pK_a Values for the pH-Dependent Transitions of Spectrin Measured by Various Techniques[a]

	no. of expt	pK_1^{app}	m	pK_2^{app}	n
A_{294}	3	10.61 ± 0.13	1	11.5 ± 0.23	2
lysine ε-CH_2 chemical shift[b]	1	10.75 ± 0.10	1	11.71 ± 0.04	2
$[\theta]_{222}$	3	10.29 ± 0.06	2	11.5 ± 0.16	2
$s_{20,w}$ (dimer)	3	9.85 ± 0.18	2	11.4 ± 0.21	2
% monomers	3	9.94 ± 0.15	2		

[a] Data shown in Figure 2 and similar experiments were fitted with eq 8 using nonlinear regression, and values of apparent pK_a for the first (pK_1^{app}) and the second transitions (pK_2^{app}) were returned (see Materials and Methods for details). m and n are the cooperativity coefficients for the first and the second transitions, respectively. The errors represent the standard deviations of the mean values for the three experiments, except for the chemical shift data where the standard error returned from the fitting process is quoted. [b] This experiment was performed in the presence of D_2O.

Correlation with Deprotonation of Tyrosine and Lysine Residues within Spectrin. Figure 4 shows a set of spin-echo ^{1}H NMR spectra of spectrin acquired at various pH values at 20 °C. The resonance at ~3 ppm at pH_{app} 7 (which predominantly represents the lysine ε-CH_2) shifted upfield as the pH was increased due to deprotonation of the side-chain amine of lysines in the relatively mobile regions of spectrin (*15*, *24*). The plot of the lysine chemical shift vs pH was fitted using eq 8 as shown in Figure 2C. The pH dependence was fitted adequately with a model representing a 2-step transition ($m = 1$, $n = 2$), and returned values of apparent pK_a are listed in Table 1. The area under the peak also increases with pH, reflecting an increase in the number of highly mobile lysine residues in the protein.

The spectrophotometric absorption maximum of tyrosine shifts from 275 to 294 nm at alkaline pH due to ionization of the hydroxyl group (*25*, *26*). On this basis, the absorbance at 294 nm of spectrin was measured as the pH was raised from 6 to 13 to monitor the ionization of tyrosyl groups in spectrin. The pH titration of tyrosine residues at 20 °C is shown in Figure 2B together with the data from the CD analysis. The plot was fitted using eq 8 with the cooperativity coefficients fixed at $m = 1$ and $n = 2$. The returned values of the apparent pK_a are listed in Table 1. The data show that the pH dependence of the absorbance resembles the plots obtained from the CD and the NMR analysis. Reversibility of the transition was examined spectrophotometrically in the ranges pH 7−11 and pH 11−13. This study indicated that the first transition was reversible, while the second transition was only partially reversible (data not shown).

No time dependence of the unfolding transitions was observed over the 2−3 h required to obtain each of the various types of titration data above.

Comparison with the Effects of Urea and High Salt. Urea (3 M) has been shown to be effective in dissociating erythrocyte spectrin oligomers into monomers (*14*). High salt (>0.3 M NaCl) has also been shown to destabilize erythrocyte spectrin heterodimers (*27*), and 2 M KI has been shown to dissociate brain spectrin oligomers into monomers

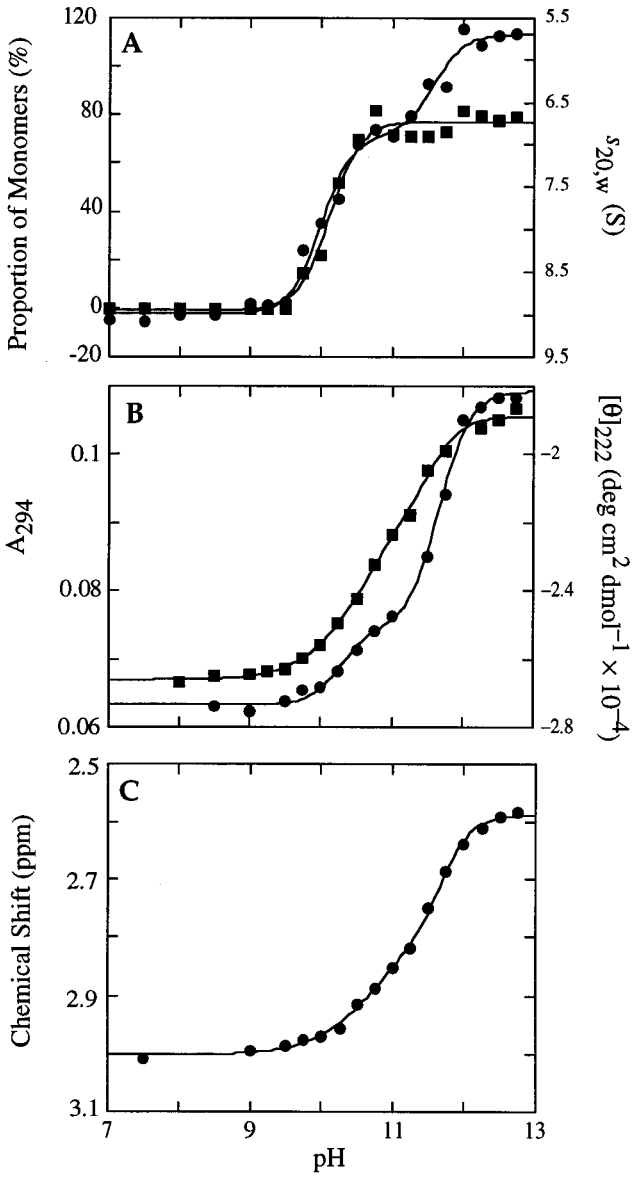

FIGURE 2: pH-dependent transitions of spectrin (0.1 g/L) detected using various biophysical techniques at 20 °C. The various plots were fitted with eq 8 in which the cooperativity coefficients were fixed at the values shown in Table 1. (A) The pH dependence of the proportion of spectrin monomers (■) and the sedimentation coefficient of spectrin heterodimer (●). Data are taken from Figure 1B and Figure 1A, respectively. (B) Spectrophotometric pH titration of tyrosine residues of spectrin at 294 nm (■) and the pH dependence of the mean residue CD ellipticity at 222 nm of spectrin (●). (C) Upfield shift of the lysine ϵ-CH_2 resonance of spectrin in D_2O detected by spin-echo ^1H NMR spectroscopy. pH values were not corrected for the presence of D_2O. Returned values of the apparent pK_a values for the transitions are listed in Table 1.

(*28*). Therefore, we have examined the effects of urea (3 M) and high salt (2.5 M NaCl) on the conformation of erythrocyte spectrin and have compared those effects with that of alkaline pH (11).

Figure 5 shows typical sets of data (scans and fits) for spectrin centrifuged (A) at pH 11, (B) in 3 M urea at pH 7.5, and (C) in 2.5 M NaCl at pH 7.5. Sedimentation velocity scans (up to 9 scans) were simultaneously fitted to a 3-species model using the program SVEDBERG (*20*), which returns estimates of the values of the sedimentation coefficients, diffusion coefficients, molecular weights, and

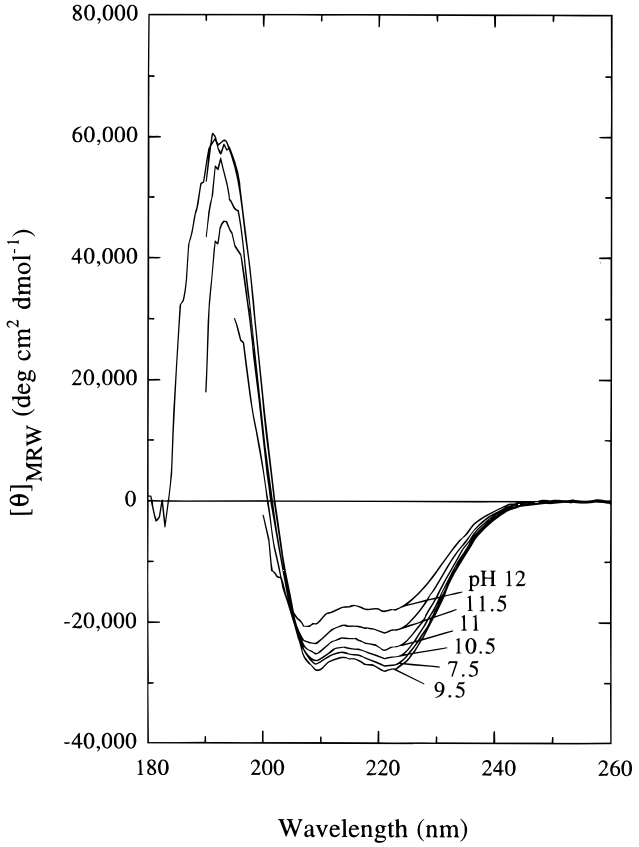

FIGURE 3: Far-UV region of the CD spectra of spectrin (0.1 g/L) acquired at pH values 7.5−12. $[\theta]_{MRW}$ is the mean residue ellipticity.

the percentage proportions of sedimenting boundaries. In general, separate sedimenting boundaries were more distinguishable over the range of alkaline pH than in urea or in high salt. Table 2 summarizes the returned values of the parameters for the three different conditions.

At pH 11, 71% of spectrin exists as monomers. The molecular mass of 199 kDa is smaller than expected (280 kDa for the α- and 246 kDa for the β-subunit) because the broadening of the sedimenting boundary resulting from the presence of two monomers of different molecular weights gives rise to a returned value of the diffusion coefficient which is larger than expected. Twenty-one percent of protein had an $s_{20,w}$ value consistent with that of the dimer at this pH, and 8% unfolded or degraded protein was present.

In 3 M urea solution, a species with $s_{20,w}$ of 6.5 S and a molecular mass of ∼300 kDa represented 65% of total protein. The $s_{20,w}$ value is too large for monomers, even in the absence of denaturant [see accompanying paper (*31*)]. In addition, the molecular weight is larger than expected for monomers, particularly given the effects of boundary broadening on the value of the diffusion coefficient. Therefore, although spectrin oligomers dissociate into monomers in 3 M urea, this sedimenting boundary probably represents a rapid equilibrium between the heterodimer and dissociated α- and β-subunits.

In 2.5 M NaCl, the major boundary (82% of solute) contained protein with an $s_{20,w}$ of 8.45 S and a molecular mass of 428 kDa. The values are smaller than expected for dimers, and the boundary probably represents dimer which is in rapid equilibrium with dissociated monomers.

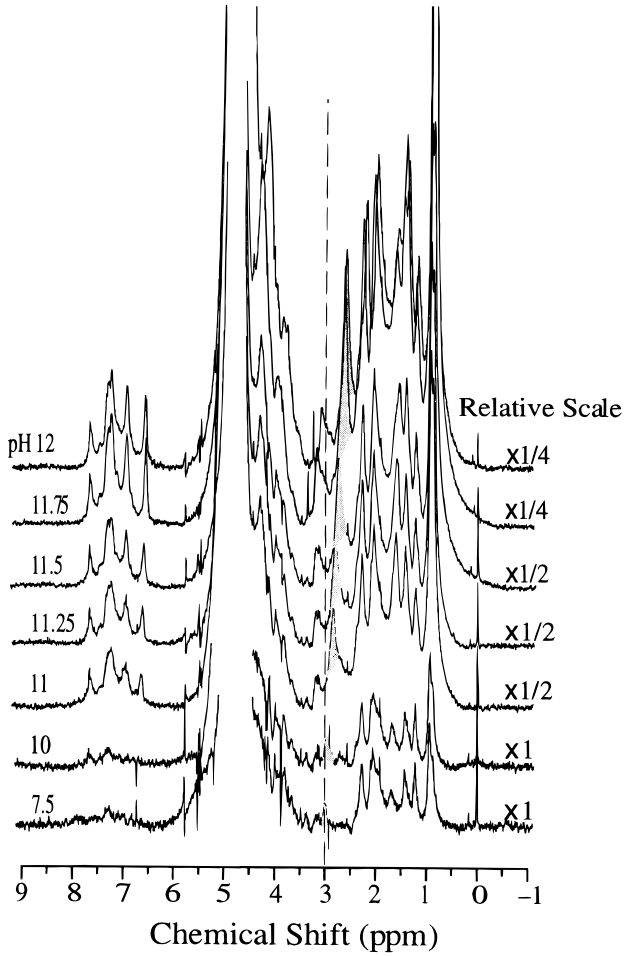

FIGURE 4: Spin-echo ^{1}H NMR spectra of spectrin acquired at pH values 7.5−12. Spectra were collected using the CPMG pulse sequence with a total echo time, τ, of 2 ms to remove the broad envelope of resonances associated with highly immobile protons. Note that the shaded peak at 3 ppm at pH 7.5, which largely represents ϵ-CH_2 protons from lysine, shifted upfield as the pH was raised.

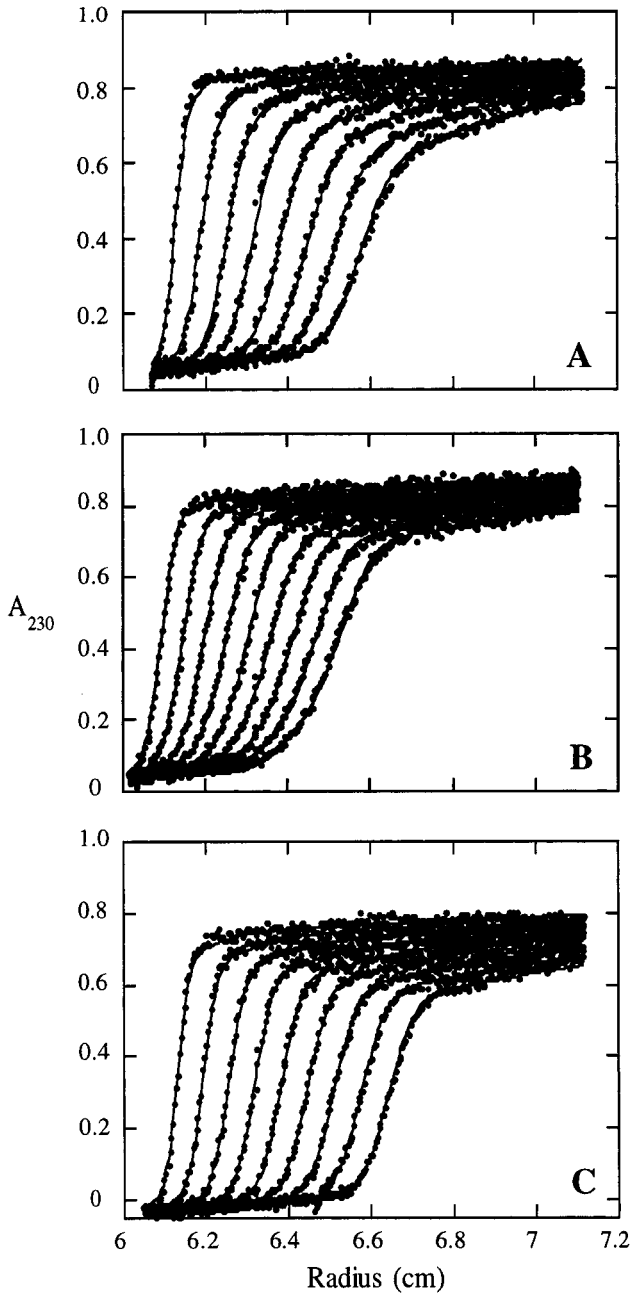

FIGURE 5: Sedimentation velocity analysis of human erythrocyte spectrin under dissociating conditions. The samples (0.1 g/L) in 50 mM sodium phosphate, 50 mM sodium borate, and 70 mM NaCl were centrifuged at (A) 46 000 rpm at pH 11, (B) 42 000 rpm in 3 M urea at pH 7.5, and (C) 46 000 rpm in 2.5 M NaCl at pH 7.5 at 20 °C. Typical sets of data are shown. Each panel shows up to 9 scans of the sedimenting boundaries recorded at 15 min intervals. The points represent the measured absorbances at 230 nm, and the lines are the best fits to a model (using the program SVEDBERG; *20*) in which three species sediment independently.

DISCUSSION

Our results show that spectrin dimers and tetramers cooperatively dissociate into α- and β-monomers above pH 9.5 (Figures 1B, 2A). This pH also marks the start of several other physical changes in the molecule. These include (i) the unfolding of spectrin, as measured by the loss of α-helix using CD measurements (Figure 2B), (ii) an increase in the number of highly mobile ϵ-CH_2 protons of lysine, as measured by spin-echo NMR (Figure 4), and (iii) the expansion in hydrodynamic shape of tetramers, dimers, and monomers, as reflected by decreasing values of their sedimentation coefficients (Figures 1A, 2A).

The dissociation of spectrin oligomers to monomers is highly cooperative and is completed by pH 10.5 (Figures 1B, 2A). The apparent pK_a is less than 10 (Table 1). The dissociation closely correlates with the first transition of the expansion in the hydrodynamic shape of the spectrin dimer (Figure 2A, Table 1). This expansion may principally reflect partial disruption of the quaternary structure of the dimers. The α- and β-subunits of a spectrin dimer interact strongly via a nucleation site which lies close to the actin-binding end of the molecule. The subunits are then envisaged to "zip up" via a series of weaker interactions which lie along the length of the two subunits (*29*). Hydrodynamic expansion of dimers and tetramers with increasing pH may then reflect partial unzipping of the subunits prior to complete dissociation.

The expansion of dimers as well as the dissociation of tetramers and dimers to monomer subunits is also accompanied by partial unfolding of the spectrin molecule, as measured by CD (Figures 2B, 3). The apparent pK_a for the first transition of unfolding is approximately 0.3 higher than the apparent pK_a values for dissociation and expansion (Table

Table 2: Sedimentation Velocity Analysis of Spectrin under Dissociating Conditions[a]

conditions		species 1	species 2	species 3
pH 11	$s_{20,w}$	7.03	4.99	2.4
	D		2.27	
	M		199	
	P	21	71	8
3 M urea	$s_{20,w}$	9.76	6.50	5.01
	D		1.73	
	M		301	
	P	6.6	65	29
2.5 M NaCl	$s_{20,w}$	11.94	8.45	4.68
	D		1.39	
	M		428	
	P	14	82	5

[a] The spectrin samples (0.1 g/L) were centrifuged at 20 °C either at (i) 46 000 rpm at pH 11, (ii) 42 000 rpm in 3 M urea, or (iii) 46 000 rpm in 2.5 M NaCl. Estimates of the values of sedimentation coefficient, $s_{20,w}$ (S), diffusion coefficient, D ($cm^2\ s^{-1} \times 10^{-7}$), and molecular weight, M (kg/mol), were obtained by fitting 8−9 sedimentation velocity scans to a 3-species model using the program SVEDBERG (*20*). P is the percentage of each species.

1). Nevertheless, a small degree of unfolding may be all that is required to effect significant dissociation. Spectrin dissociation is especially sensitive to apparently minor changes in structure. For example, point mutations removed by several repeat units (up to 200 Å) from the tetramerization interface can nevertheless disrupt polymerization (*30*). The unfolding of spectrin will also contribute to the hydrodynamic expansion of the molecule.

The dissociation, expansion, and unfolding of spectrin are most likely due to the deprotonation of tyrosine and lysine residues within spectrin (Figures 2B, C). Deprotonation is biphasic for both types of residue. In the case of tyrosine residues, the first phase (up to pH 11) is fully reversible, while the second phase is not (Figure 2B). The second transition most probably reflects those tyrosines buried more deeply in the hydrophobic core of the triple-helical bundles of the repeat motifs.

The first phase of the deprotonation of tyrosine residues has an apparent pK_a value ∼0.6 unit higher than that for dissociation and expansion. Again, it is probable that the deprotonation of a small subset of tyrosines is sufficient to produce dissociation of tetramers and dimers to monomer subunits and result in some unfolding of the protein. Our data cannot be used to determine the exact location of this subset of tyrosines, but several possibilities exist. In particular, tyrosine is relatively conserved at position 30 of the spectrin α-subunit repeats which places it in the AB loop (residue numbering taken from Yan *et al.* (*9*)). These tyrosines are likely to be relatively exposed to solvent and therefore have relatively low pK_a values. Their conservation suggests that they play an important role in the structure/function of the molecule, and their deprotonation may be sufficient to disrupt association and promote unfolding.

Lysine residues also deprotonate in the same pH range as tyrosine (Table 1). The X-ray structure of a single repeat motif (*9*) shows the presence of several salt bridges involving lysine both within and between the three helices of the bundle. These would appear to be important in stabilizing the triple-helical fold. In addition, lysine is conserved at several positions in repeat motifs of both the α- and β-subunits with some of these positions (e.g., A21 in both the α- and β-subunits repeats and C25 in the α-subunit repeats) being within the hydrophobic core of the triple-helical bundle. Deprotonation of lysines would then disrupt both the salt bridges formed by this residue and the associated stability of the repeat motif fold.

Our spin-echo NMR spectra also show that the peak ascribed to ϵ-CH_2 of lysine increases in area with increasing pH (Figure 4). The areas are difficult to quantify, but there appear to be two transitions with the apparent pK_a of the first being in the range 10−11. The spin-echo NMR experiments detect only highly mobile protons, most of which are believed to reside in random coil segments of the protein (*15*). An increase in area for this peak then reflects, to a large degree, an increasing number of lysine residues in random coil segments of the protein. That is, increasing pH results in unfolding which correlates with dissociation and hydrodynamic expansion of spectrin.

We used sedimentation velocity to analyze the dissociation of spectrin at pH 11, in 3 M urea, and in 2.5 M NaCl (Table 2). Each of these methods is known to at least partly dissociate spectrin to monomer subunits, and 3 M urea is used to purify spectrin subunits (*14*, *27*; Figures 1, 2). At pH 11, the major component (∼70% of material) appeared to be monomeric. A component representing ∼20% of material which had a sedimentation coefficient consistent with that of dimer at this pH was also present. This subset of dimers is apparently refractory to dissociation, and the possible reasons for this are discussed in the accompanying paper (*31*). Very little (<10%) of the material appeared to be degraded or highly unfolded.

In contrast, the main component of spectrin (∼65% of material) in the presence of 3 M urea appeared to be an equilibrium between monomers and dimer. This would increase the difficulty of separating and purifying the individual subunits and would probably result in reduced yields. A similar situation occurs in the presence of 2.5 M NaCl, but with the equilibrium shifted even further toward the dimer.

Of particular importance to the pH-dependent dissociation of spectrin is the observation that the first transition (up to pH 11), as measured by the absorbance at 294 nm, is reversible. This shows that the unfolding of the protein that accompanies deprotonation of both tyrosines and lysines is also reversible. Since dissociation to the monomer subunits is largely completed by pH 10.5, the results suggest that manipulating pH can be used to aid in the purification of α- and β-subunits of spectrin. Fujita *et al*., in the accompanying paper (*31*), discuss this purification process and examine the biophysical properties of the individual subunits and their recombination into functional heterodimers and tetramers. This purification scheme is a more reliable and simpler alternative to the commonly used method employing urea (*14*).

ACKNOWLEDGMENT

We would like to thank Gillian Begg, Alissa Henniker, and Lisa Joss for helpful discussions. Greg Ralston died on Aug 20, 1997. He will be remembered as a highly valued colleague and friend to many researchers worldwide.

REFERENCES

1. Bennett, V., and Gilligan, M. D. (1993) *Annu. Rev. Cell Biol. 9*, 27−66.
2. Waugh, R. E., and Agre, P. (1988) *J. Clin. Invest. 81*, 133−141.
3. Elgsaeter, A., Stokke, B. T., Mikkelsen, A., and Branton, D. (1986) *Science 234*, 1217−1223.
4. Sahr, K. E., Laurila, P., Kotula, L., Scarpa, A. L., Coupal, E., Leto, T. L., Linnenbach, A. J., Winkelmann, J. C., Speicher, D. W., Marchesi, V. T., Curtis, P. J., and Forget, B. G. (1990) *J. Biol. Chem. 265*, 4434−4443.
5. Winkelmann, J. C., Chang, J. G., Tse, W. T., Scarpa, A. L., Marchesi, V. T., and Forget, B. G. (1990) *J. Biol. Chem. 265*, 11827−11832.
6. Speicher, D. W. (1986) *J. Cell. Biochem. 30*, 245−258.
7. McGough, A. M., and Josephs, R. (1990) *Proc. Natl. Acad. Sci. U.S.A. 87*, 5208−5212.
8. Shotton, D. M., Burke, B. E., and Branton, D. (1979) *J. Mol. Biol. 131*, 303−329.
9. Yan, Y., Winograd, E., Viel, A., Cronin, T., Harrison, S. C., and Branton, D. (1993) *Science 262*, 2027−2030.
10. Speicher, D. W., and Ursitti, J. A. (1994) *Curr. Biol. 4*, 154−157.
11. Liu, S. C., Windisch, P., Kim, S., and Palek, J. (1984) *Cell 37*, 587−594.
12. Speicher, D. W., DeSilva, T. M., Speicher, K. D., Ursitti, J. A., Hembach, P., and Weglarz, L. (1993) *J. Biol. Chem. 268*, 4227−4235.
13. Tse, W. T., Lecomte, M.-C., Costa, F. F., Garbarz, M., Fero, C., Boivin, P., Dhermy, D., and Forget, B. G. (1990) *J. Clin. Invest. 86*, 909−916.
14. Yoshino, H., and Marchesi, V. T. (1984) *J. Biol. Chem. 259*, 4496−4500.
15. Begg, G. E., Ralston, G. B., and Morris, M. B. (1994) *Biophys. Chem. 52*, 63−73.
16. Low, P. S., Westfall, M. A., Allen, D. P., and Appell, K. C. (1984) *J. Biol. Chem. 259*, 13070−13076.
17. Gill, S. G., and von Hippel, P. H. (1989) *Anal. Biochem. 182*, 319−326.
18. Ralston, G. B. (1976) *Biochim. Biophys. Acta 455*, 163−172.
19. Sommerville, L. E., Henry, G. D., Sykes, B. D., and Hartshorne, D. J. (1990) *Biochemistry 29*, 10855−10864.
20. Philo, J. S. (1994) in *Modern Analytical Ultracentrifugal Analysis* (Schuster, T. M., and Laue, T. M., Eds.) pp 156−170, Birkhauser, Boston, Secaucus, NJ.
21. Tanford, C. (1961) *Physical Chemistry of Macromolecules*, pp 526−586, Wiley, New York.
22. Ellis, K. J., and Duggleby, R. G. (1978) *Biochem. J. 171*, 513−517.
23. Chen, Y.-H., Yang, J. T., and Chan, K. H. (1974) *Biochemistry 13*, 3350−3359.
24. Highsmith, S., Akasaka, K., Konrad, M., Goody, R., Holmes, K., Wade-Jardetzky, N., and Jardetzky, O. (1979) *Biochemistry 18*, 4238−4244.
25. Herskovits, T. T. (1967) *Methods Enzymol. 11*, 748−775.
26. Tanford, C. T., Hauenstein, J. D., and Rands, D. G. (1956) *J. Am. Chem. Soc. 77*, 6409−6413.
27. Cole, N., and Ralston, G. B. (1992) *Biochim. Biophys. Acta 1121*, 23−30.
28. Glenney, J. R., Jr., and Weber, K. (1985) *Anal. Biochem. 150*, 364−368.
29. Speicher, D. W., Weglarz, L., and DeSilva, T. M. (1992) *J. Biol. Chem. 267*, 14775−14782.
30. Delaunay, J., and Dhermy, D. (1993) *Semin. Hematol. 30*, 21−33.
31. Fujita, T., Ralston, G. B., and Morris, M. B. (1998) *Biochemistry 37*, 272−280.

BI971966Z